

Application and evaluation of a snowmelt runoff model in the Tamor River basin, Eastern Himalaya using a Markov Chain Monte Carlo (MCMC) data assimilation approach

Prajjwal K. Panday,^{1*} Christopher A. Williams,² Karen E. Frey² and Molly E. Brown³

¹ Woods Hole Research Center, 149 Woods Hole Road, Falmouth, MA, 02540, USA

² Graduate School of Geography, Clark University, 950 Main Street, Worcester, MA, 01610, USA

³ Biospheric Sciences, NASA Goddard Space Flight Center, Greenbelt, MD, 20771, USA

Abstract:

Previous studies have drawn attention to substantial hydrological changes taking place in mountainous watersheds where hydrology is dominated by cryospheric processes. Modelling is an important tool for understanding these changes but is particularly challenging in mountainous terrain owing to scarcity of ground observations and uncertainty of model parameters across space and time. This study utilizes a Markov Chain Monte Carlo data assimilation approach to examine and evaluate the performance of a conceptual, degree-day snowmelt runoff model applied in the Tamor River basin in the eastern Nepalese Himalaya. The snowmelt runoff model is calibrated using daily streamflow from 2002 to 2006 with fairly high accuracy (average Nash–Sutcliffe metric ~ 0.84 , annual volume bias $< 3\%$). The Markov Chain Monte Carlo approach constrains the parameters to which the model is most sensitive (e.g. lapse rate and recession coefficient) and maximizes model fit and performance. Model simulated streamflow using an interpolated precipitation data set decreases the fractional contribution from rainfall compared with simulations using observed station precipitation. The average snowmelt contribution to total runoff in the Tamor River basin for the 2002–2006 period is estimated to be $29.7 \pm 2.9\%$ (which includes $4.2 \pm 0.9\%$ from snowfall that promptly melts), whereas $70.3 \pm 2.6\%$ is attributed to contributions from rainfall. On average, the elevation zone in the 4000–5500 m range contributes the most to basin runoff, averaging $56.9 \pm 3.6\%$ of all snowmelt input and $28.9 \pm 1.1\%$ of all rainfall input to runoff. Model simulated streamflow using an interpolated precipitation data set decreases the fractional contribution from rainfall *versus* snowmelt compared with simulations using observed station precipitation. Model experiments indicate that the hydrograph itself does not constrain estimates of snowmelt *versus* rainfall contributions to total outflow but that this derives from the degree-day melting model. Lastly, we demonstrate that the data assimilation approach is useful for quantifying and reducing uncertainty related to model parameters and thus provides uncertainty bounds on snowmelt and rainfall contributions in such mountainous watersheds. Copyright © 2013 John Wiley & Sons, Ltd.

Supporting information may be found in the online version of this article.

KEY WORDS snowmelt; hydrology; SRM; APHRODITE; MODIS snow; Himalaya; MCMC; data assimilation

Received 11 January 2013; Accepted 6 August 2013

INTRODUCTION

Growing evidence indicates that the low-latitude mountainous cryosphere is undergoing change owing to recent warming (IPCC, 2007; Yao *et al.*, 2012). Geographic areas where the water cycle is dominated by snowmelt hydrology are expected to be more susceptible to climate change, as it affects the seasonality of runoff (Barnett *et al.*, 2005; Adam *et al.*, 2009). The Hindu Kush–Himalaya (HKH), regarded as the ‘water towers’ of Asia, is one such critical region as it nourishes several of the major Asian watersheds through perennial rivers such as the Ganges, Indus and Brahmaputra (Messerli *et al.*, 2004). Most recent research analyzing

tropospheric temperatures from the longest available record of microwave satellite measurements reveals widespread pre-monsoonal and mean annual warming over the HKH region at a rate of 0.21 ± 0.08 °C/decade (Gautam *et al.*, 2010). Regional climate projections by the Intergovernmental Panel on Climate Change (IPCC, 2007) indicate Central Asia may warm by a median temperature of 3.7 °C by the end of the 21st century, with warming over high altitudes across the HKH (Panday *et al.*, in review). There is an increasingly large body of evidence of a glacio-hydrological response along the east–west transect of the HKH corresponding to these climatic changes, with glaciers in the Eastern Himalaya exhibiting retreat and negative mass balance and glaciers in the Karakoram and northwestern Himalaya exhibiting a positive mass balance over the last few decades (Bolch *et al.*, 2012; Yao *et al.*, 2012). Such climate-driven responses of mountainous river

*Correspondence to: Prajjwal K. Panday, Woods Hole Research Center, 149 Woods Hole Road, Falmouth, MA, 02540, USA.
E-mail: ppanday@whrc.org

hydrology may pose significant challenges for this region. Despite its regional importance and vulnerability to climate change, there is uncertainty associated with the physical processes that control runoff generation at high altitudes (Bolch *et al.*, 2012; Pellicciotti *et al.*, 2012) and subsequently with the rates and magnitude of climate change impacts on snow cover and snowmelt hydrology.

Water resource management and the evaluation of impacts of climatic change require quantification of streamflow variability. Hydrological models provide a framework to investigate these relationships and subsequently use a scenario approach to evaluate projections of hydrological variables (Maurer *et al.*, 2009). The assessment of hydrological impacts of climate change is particularly challenging in mountainous environments as they constitute complex hydrological systems owing to extreme heterogeneity in vegetation, soils, topography and spatially and temporally varying snow cover and snowmelt patterns (Gurtz *et al.*, 2005; Panday *et al.*, 2011). Continued efforts in hydrological modelling of snow and glacier melt in the HKH region mostly through conceptually lumped, semi-distributed (rather than physically based models) have provided baseline patterns of spatiotemporal patterns of precipitation and runoff at very large scales (Bookhagen and Burbank, 2010; Immerzeel *et al.*, 2010). However, poor accessibility and scarcity of adequate network of hydrometeorological stations at high altitude regions still remain a major impediment to runoff modelling. As a result, only a few studies have explored snowmelt runoff models at the catchment or river-basin scale in this region (Braun *et al.*, 1993; Shrestha *et al.*, 2004; Akhtar *et al.*, 2008; Tahir *et al.*, 2011).

Parameterization is usually challenging owing to scarcity of data in mountainous regions such as the HKH, and a sound understanding of the snowmelt hydrology needs to be emphasized prior to assessment of water resources in a changing climate. Several catchment-scale and basin-scale modelling studies have addressed the glacio-hydrological processes in the Himalayan region (Konz *et al.*, 2007; Akhtar *et al.*, 2008; Butt and Bilal, 2011; Immerzeel *et al.*, 2011; Tahir *et al.*, 2011). A majority of these studies have adopted parameter values from the literature without rigorous calibration and without quantifying how parameter uncertainty influences modelled results. Transfer of parameters across space and time in hydrological modelling can be problematic, particularly in conceptual models of snowmelt when parameters either do not have a physical meaning or are not easily measurable (Sun *et al.*, 2012). In order to address the issues of parameterization and model uncertainty, data assimilation methods are typically applied in hydrology to integrate different datasets, combine model outputs with observations, update hydrological models, quantify model uncertainties and sensitivity and/or improve model accuracy (Beven and Freer, 2001; Clark *et al.*, 2006). Data assimilation can be viewed as a method to use

observations to constrain models with the goal of providing better understanding of the underlying processes (McLaughlin *et al.*, 2005). The Bayesian approach in hydrological applications allows to systematically incorporate prior information on model parameters in the data assimilation framework (Zobitz *et al.*, 2011) and to compute probability distributions of modelled outputs and characterize uncertainty in the model, usually through Monte Carlo simulation (Mishra, 2009). This provides a means of objectively and quantitatively diagnosing the parameters and processes to which a model is most sensitive and from which one can learn. Few studies have emphasized the need for parameterization in the Himalayan region and have performed extensive calibration (Konz *et al.*, 2007; Immerzeel *et al.*, 2011; Pellicciotti *et al.*, 2012) and validation with additional data sets such as glacier mass balances and remotely sensed snow cover. Pellicciotti *et al.* (2012) also emphasized that an assessment of the internal consistency of the model is important owing to the problem of multiplicity of parameter sets or equifinality.

In addition to parameter uncertainty, sensitivity of hydrological models to input data such as precipitation also needs to be evaluated particularly in complex topography and high elevations. Hydrological models in mountainous regions with scarce observations are usually forced with precipitation data located at lower altitudes, which can introduce added uncertainty. Satellite-derived precipitation estimates and interpolated rain-gauge observations have been used in other studies as inputs to a snowmelt runoff model (SRM) instead of gauged precipitation. Bookhagen and Burbank (2010) used improved Tropical Rainfall Measuring Mission rainfall estimates to characterize the spatiotemporal distribution of rainfall, snowfall and evapotranspiration across the Himalayan region, whereas Tahir *et al.* (2011) successfully used interpolated daily precipitation data to simulate snowmelt hydrology in the Hunza River basin.

A thorough assessment of hydrologic processes, patterns and trends requires minimization of uncertainties in modelling and available input data. The objective of this study is to examine spatial and temporal variations in snowmelt contributions to runoff in the Hindu Kush-Himalayan region and Tamor River basin by using a data assimilation approach that both combines available input data with a degree-day based SRM and estimates model parameters by using a Markov Chain Monte Carlo (MCMC) technique. Additionally, we investigate and evaluate the performances of the SRM when driven by observed precipitation as well as interpolated gridded precipitation data. We demonstrate how a data assimilation approach can be coupled with a SRM to investigate the issues of model parameter sensitivity and uncertainty and improve performance in a data-scarce basin in the Eastern Himalaya.

METHODS

Study area

This geographic domain of this study is the upstream portion of the Tamor River basin in the Eastern Himalaya of Nepal (Figure 1). The Tamor basin covers an area of 4274 km², with an elevation range of 422 to 8505 m (Figure 2). The Tamor River, which is one of the major tributaries of the Sapta Koshi River, flows between high peaks such as Kanchenjunga (8586 m) and Everest (8848 m) on gorges reaching depths of 2000 m. Precipitation for the region is highly seasonal and concentrated during the summer monsoon months (June to September) (Figure 3). The upper reaches of the basin are snow covered and glaciated, contributing melt water to streamflow.

Hydrometeorological data

Hydrometeorological measurements for the Tamor River basin in the Eastern Himalaya were acquired from the Department of Hydrology and Meteorology, Nepal. Daily temperature data at Taplejung station (27.35°N, 87.67°E at 1732 m elevation) and daily precipitation data measured at Lunghung station (27.55°N, 87.78°E at 1780 m elevation) in the Taplejung district were used for the hydrological modelling (Figure 1). Discharge data measured daily from 2002–2006 for the Tamor River at Majhitar station (27.15°N, 87.71°E at 533 m elevation) were used for calibration. The Tamor basin was delineated at the Majhitar station using the 90 m digital elevation data

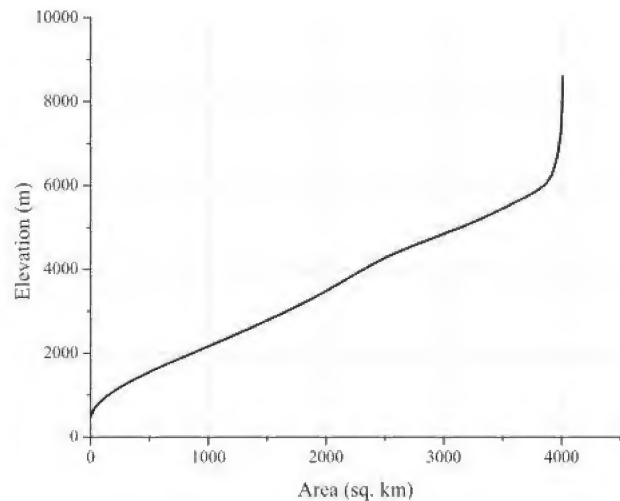


Figure 2. Area-elevation curve for the Tamor River basin

acquired from the Consultative Group on International Agricultural Research–Consortium for Spatial Information. The basin was divided into four zones, and the zonal mean hypsometric elevation (Figure 2) was used as the elevation to which base station temperatures were extrapolated for the calculation of zonal degree days (Table I).

Moderate Resolution Imaging Spectroradiometer (MODIS) snow cover

Satellite-derived snow cover is the most efficient and readily available input for snowmelt runoff modelling. Snow cover was derived using the MODIS/Terra Snow

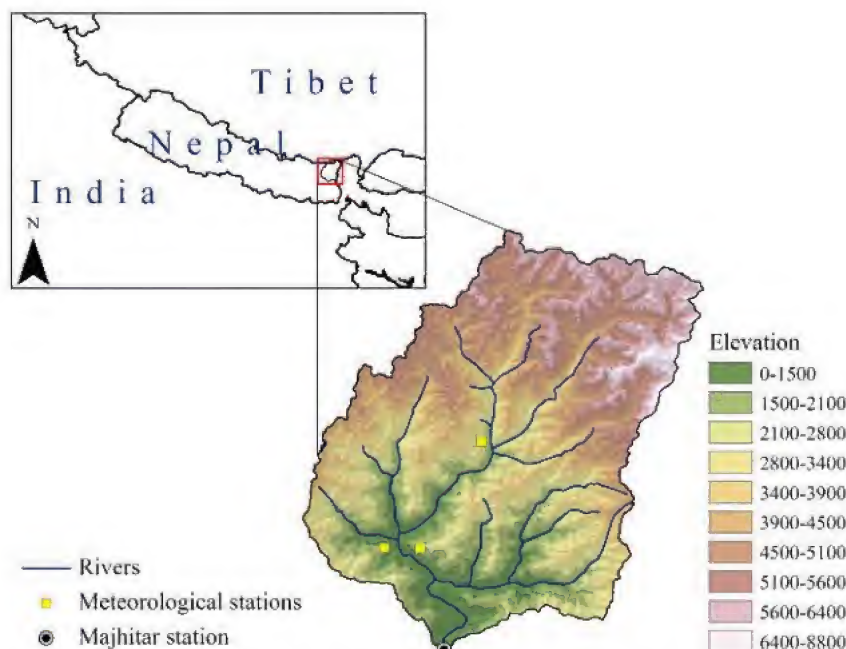


Figure 1. Location and topography of the Tamor River basin in the eastern Nepalese Himalaya

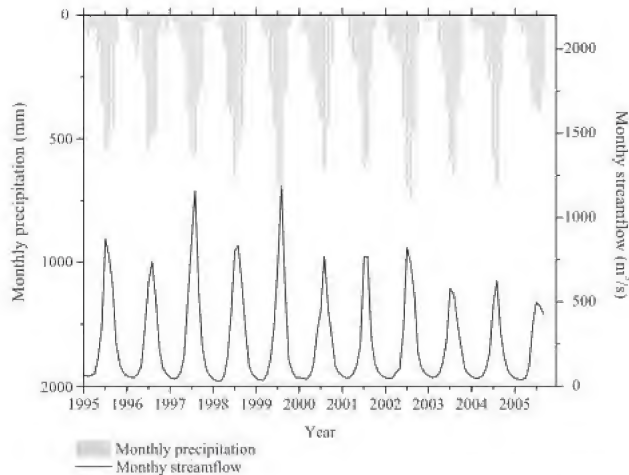


Figure 3. Average monthly streamflow (m^3/s) and total monthly precipitation (mm) from 1996 to 2006 at Majhitar station

Table I. Elevation zone, elevation range, mean elevation and zonal area for the four zones of the Tamor River basin

Elevation zone	Elevation range (m)	Mean elevation of zone (m)	Zonal area (km^2)
1	533–2500 m	1685.9	1355.5
2	2500–4000 m	3208.1	1111.3
3	4000–5500 m	4764.3	1297.9
4	>5500	5988.8	509.2
Total basin	—	—	4273.8

Cover 8-Day L3 Global 500 m Grid (MOD10A2; Hall *et al.*, 2006) and updated every eight days using a snow depletion curve. The MODIS snow cover is based on a snow mapping algorithm that uses at-satellite reflectance in MODIS bands 4 (0.545–0.565 μm) and 6 (1.628–1.652 μm) to compute the Normalized Snow Difference Index (Hall *et al.*, 2002). A pixel will be mapped as snow if the Normalized Snow Difference Index ≥ 0.4 and MODIS band 2 (0.841–0.876 μm) $> 11\%$; however, if the MODIS band 4 reflectance is $< 10\%$, the pixel will not be mapped as snow even if the other criteria are met. The MODIS product distributed through the National Snow and Ice Data Centre was acquired for the scene h25v06, covering the study region from 2002 to 2006. The MODIS images were reprojected to Universal Transverse Mercator zone 45 projection system, and the Tamor River basin area was then extracted to assess the fraction of snow cover for different altitudinal zones. Average snow cover was estimated by interpolating linearly between the previous and next available cloud free images for days with cloud cover following Tahir *et al.* (2011). The conventional depletion curves were derived for each elevation zone using the 8-day snow cover data, which provide the input to the SRM as the decimal portion of snow-covered area for each day.

Asian Precipitation \square Highly Resolved Observational Data Integration towards Evaluation (APHRODITE) precipitation data

Spatially representative gridded precipitation data are also used to drive a snowmelt runoff model, as valley stations may not be representative for basin precipitation. The APHRODITE of the water resources project has compiled a daily gridded precipitation dataset covering 1951–2007 period by analyzing rain-gauge observation data across Asia (Yatagai *et al.*, 2009). The APHRODITE data used in this research (APHRO_MA_V1003R1) have a $0.25 \times 0.25^\circ$ gridded spatial resolution, which was interpolated from meteorological stations throughout this region. Whereas satellite data consistently underestimate or overestimate the amount of precipitation, particularly in the monsoon season (Duncan and Biggs, 2012), APHRODITE data have been shown to provide the best precipitation estimates in most regions except at high elevations where accuracy of this data set is limited (Andermann *et al.*, 2011). We used the basin-averaged APHRODITE precipitation as input to the SRM assuming it to be constant across elevation zones. The model was run using APHRODITE precipitation data to determine the reliability of the dataset for snowmelt runoff modelling in the Tamor River basin.

Snowmelt runoff modelling

Modelling of stream discharge was based on the SRM developed by Martinec *et al.* (2008). SRM is a conceptual, deterministic, degree-day hydrological model that simulates and forecasts daily runoff resulting from snowmelt and precipitation from hydrometeorological input data. The model was designed for streamflow modelling in basins where snowmelt is a major contributor, and more recently, it has been applied for evaluation of impacts of climate change on seasonal snow cover and runoff (Immerzeel *et al.*, 2010). SRM has been applied to basins ranging from 0.76 to 917 444 km^2 and across elevation ranges from 0 to 8840 m in over 100 basins in 29 different countries (Martinec *et al.*, 2008). This model was chosen in this study to assess snowmelt hydrology owing to its minimal data requirements and transferability to a variety of geographic regions. On the basis of the input of daily temperature, precipitation and snow-covered area values, SRM computes the daily streamflow as

$$Q_{n+1} = C s_{zn} a_{zn} T_n + T_{zn} S_{zn} \quad (1)$$

$$C r_{zn} P_{zn} A_z \frac{10000}{86400} \square \square k_{n+1} \square \\ \square Q_n k_{n+1}, \\ k_{n+1} \square x Q_n^y \quad (2)$$

where Q (m^3/s) is discharge at day $n+1$, C is the runoff coefficient to snowmelt (Cs_n) and to rain (Cr_n) for each zone

(subscript z), a ($\text{cm}/^{\circ}\text{C}/\text{day}$) is the degree-day factor, $T + \Delta T$ ($^{\circ}\text{C}$) are the degree days, P (cm) is the precipitation per day, A (km^2) is the area of the basin, S is the fractional snow cover and k is the discharge recession coefficient. The daily average streamflow on day $n+1$ is computed by addition of snowmelt and precipitation that contributes to runoff with the discharge on the preceding day. The snowmelt of the preceding day is a product of the degree-day factor (a), zonal degree days ($T + \Delta T$) and the snow-covered area percentage (S). The snowmelt runoff coefficient (C_s) and the zonal area (A) are further multiplied with the previous product to compute the percentage that contributes to runoff. Similarly, the product of the rainfall runoff coefficient (C_r) and the zonal area (A) determines the precipitation contribution to runoff. The recession coefficient (k) is also an important parameter as it describes the structure of the falling limb of the hydrograph and correspondingly determines the proportion of daily melt water production that appears immediately in the runoff. This is obtained with analysis of historical discharge data based on Equation 2, where parameters x and y are derived by analyzing discharge on a given day as a function of the value on the previous day.

A critical temperature is used to determine whether a precipitation event is rain or snow over different parts of the basin. When precipitation is determined to be snow, its contribution to runoff depends on whether it falls on a snow-covered or previously snow-free area. Snowfall on snow-covered areas is assumed to become part of the seasonal snowpack, its depth is not tracked further, and its contribution to runoff is determined by the snow depletion curve. Daily snowmelt depth from snow-covered areas is determined on the basis of degree days and a factor that converts this to mass release, qualitatively representing the maximum potential melt given the energy input. In contrast, snow falling as precipitation over snow-free areas is accumulated until the next day warm enough to produce melting at which time it is depleted on the basis of the degree-days approach. During the winter half year (October–March), the model cancels any existing storage of preceding temporal snowfalls when snow cover is maximum such that snow on previously snow-free areas becomes part of the seasonal cover. When precipitation is considered to be rain during the cold season, rainfall runoff contributes to total runoff only from the snow-free area, and the rainfall depth is reduced by the ratio of snow-free area to zonal area. At a later stage during the season, which is set to April 1, rain falling on snow-covered areas is allowed to fully contribute to runoff such that rain from entire zonal area is accounted. The SRM approach estimates fractional contributions to total discharge from (1) daily snowmelt from the snowpack for each elevation, (2) the melt of precipitation delivered as snow but to areas described as snow-free at the time of snowfall and (3) zonal rainfall. Contributions of each to total river flow are estimated prior

to accounting for losses via runoff coefficients, introducing an implicit assumption that fractional contributions to runoff are proportional to the relative abundance of each input.

Equation (1) is applied to each zone of the basin, and total discharge is computed as sum of all zonal discharges. The SRM structure as applied in this study assumes a time lag between the daily temperature cycle and the resulting discharge cycle of 18 h. The use of this time lag is supported by the expected relation between lag time and basin size as shown in a SRM intercomparison report by the World Meteorological Organization (1986). Although the time lag parameter can be adjusted to improve synchronization of simulated and observed peaks of average daily flows, calibration of the recession coefficients provides a similar effect (Martinec *et al.*, 2008). The parameters for runoff coefficients, lapse rate, critical temperature, recession coefficient and degree-day factors reflect characteristics at a basin scale and are determined in this study with an MCMC data assimilation by maximizing the fit between the observed and modelled streamflows. The modelled streamflow is assessed for accuracy using the Nash–Sutcliffe (NS) statistic and the volume difference (D_v), where volume difference demonstrates bias. (Supplementary information, A) (Martinec *et al.*, 2008).

Model calibration using MCMC optimization

A data assimilation technique known as a MCMC routine (Zobitz *et al.*, 2011) was used to explore the parameter spaces in the SRM. The applicability of Bayesian methods in hydrological studies has increased owing to their use in parameter estimations and uncertainty assessments (Smith and Marshall, 2008). The MCMC algorithm is one of several data assimilation techniques and uses the Metropolis Hastings algorithm (Metropolis *et al.*, 1953), which iteratively adjusts the model parameters to yield the best match between the observed and modelled streamflow. The output provides a set of accepted parameter values and information about the posterior distributions of the parameters consistent with the prior information, model structure and observations. Additional details of the MCMC algorithm used for optimization are described more fully in Supplementary information, B and in Zobitz *et al.* (2011) and Braswell *et al.* (2005).

Based on the literature and range of parameter values used in other snowmelt runoff models in the HKH region (Immerzeel *et al.*, 2010; Butt and Bilal, 2011; Tahir *et al.*, 2011), we first specified prior ranges for the parameters. Table II shows the parameters with the prior ranges that were assigned seasonally or annually across different elevation zones. Seasonally varying parameters were optimized for the snowmelt and monsoon period (June–August) and the snow accumulation and dry period (September–May). Snowmelt and rainfall runoff coefficients were varied seasonally and by elevations informed by Tahir *et al.* (2011)

Table II. Initial parameter ranges used for Markov Chain Monte Carlo data assimilation

Parameter		Parameter ranges across each elevation zone			
		Zone 1 (533–2500 m)	Zone 2 (2500–4000 m)	Zone 3 (4000–5500 m)	Zone 4 (>5500 m)
Snow runoff coefficient	June–August	0.3–0.8	0.3–0.8	0.3–0.8	0.3–0.8
	September–May	0.3–0.8	0.3–0.8	0.3–0.8	0.3–0.8
Rainfall runoff coefficient	June–August	0.3–0.8	0.3–0.8	0.3–0.8	0.3–0.8
	Sep–May	0.3–0.8	0.3–0.8	0.3–0.8	0.3–0.8
Degree-day factor (cm/°C/day)	Annual	0.3–0.6	0.3–0.6	0.5–0.9	0.5–0.9
Lapse rate (°C/100 m)	Annual	0.5–0.7			
Critical temperature (°C)	Annual	0.0–2.0			
x coefficient	Annual	0.9–1.4			
y coefficient	Annual	0.0–0.25			

Snowmelt and monsoonal months are June–August, and September–May is the snow accumulation and dry period. Lapse rate, critical temperature and x and y coefficients are not varied across elevation zones.

and were assigned equal prior parameter ranges. Although degree-day factors tend to vary with different seasons, climate and surfaces, under similar conditions they are expected to increase with increasing elevation (Hock, 2003). Similar to previous studies (Butt and Bilal, 2011; Tahir *et al.*, 2011), which utilize a degree-day factor that increases with elevation, we also increase the parameter range gradually across elevation zones. The elevation zone greater than 5500 m, which are glacier and ice covered are assumed to have a higher degree-day factor as the values tend to be considerably higher for ice compared with snow (Hock, 2003). Parameters such as lapse rate, critical temperature and x and y coefficients were calibrated annually. Other studies using SRM have used a similar variation of parameters. Although most parameters can potentially vary across elevations and seasons, increasing parameter sets increase potential ranges of parameter values and thereby increase uncertainty (Seibert, 1997). For this study, we implemented the MCMC technique using three chains, each of which consisted of 10 000 iterations. The best parameter values from these chains were used in the final set of 10 000 iterations, which is used to determine the parameter distributions. The range of parameter values was deliberately set to be large at first to examine if realistic parameter values were selected by the MCMC technique. If the posterior parameter distributions were less plausible, the parameter ranges were logically constrained by literature values to be more realistic. The snowmelt and rainfall runoff coefficients were constrained in the ranges specified in Table II based on Tahir *et al.* (2011) and Butt and Bilal (2011), degree-day factor ranges were specified on the basis of Hock (2003), and prior ranges for lapse rate and critical temperature were specified from Tahir *et al.* (2011) and Butt and Bilal (2011). The SRM was run via MCMC with prior parameter ranges as specified in Table II for the hydrological years 2002 to 2006.

Model sensitivity and uncertainty

In addition to model calibration, we also carried out several experimental runs. The model was allowed to calibrate via MCMC by setting the snowmelt runoff coefficients to zero such that snowmelt contributions were neglected in the simulation of the hydrograph. Similarly, the rainfall runoff coefficients were also set to zero such that rainfall contributions were excluded in the final simulation of the hydrograph. In addition to these experiments, we conducted additional sensitivity and uncertainty analyses via ensemble streamflow simulations (1000 runs) to identify parameters that control model performance and uncertainties in modelled streamflow and total input contributions. Parameter sensitivity and uncertainty in streamflow in the time history were analyzed as 5% and 95% confidence intervals of the ensemble runs. First, we generated an ensemble of model runs ('best ensemble' hereafter) from the posterior distribution of accepted parameter sets from MCMC that represent the most likely set of parameters. Second, the sensitivity to parameters was tested by perturbing the distribution of a parameter by some amount and computing the corresponding changes in model output while preserving the distribution of other parameters. This is performed in this study by randomly drawing from the altered distribution of each parameter (e.g. $\pm 10\%$ from the mean value of a parameter from the posterior distribution) to generate ensemble runs. This allows quantifying the effects of each parameter or a combination of parameters on model output and on total input contributions to streamflow by providing uncertainty bounds on the output statistics. Third, an ensemble of parameter sets was generated by randomly sampling from the cumulative distribution curve constructed from the posterior distribution of each parameter. The ensemble model simulation uses the full range of parameter variations and combinations and thereby provides overall uncertainties in the choice of model parameters generated from MCMC.

RESULTS

Summary of meteorological parameters

Long term annual temperatures (1970–2006) at the Taplejung station averaged 16.3 °C, whereas average winter and summer temperatures were 10 °C and 21.3 °C, respectively. Mann–Kendall tests indicate significant ($p < 0.05$) positive trends in both annual maximum and average temperatures for the Taplejung station during this period. Average annual precipitation at the Lungthung station was ~2484 mm for the 1996–2006 period. On average, approximately 76% of the precipitation is received during the summer monsoon. The monthly streamflow for the Tamor River basin at the Majhitar station along with the total monthly precipitation at Lungthung station indicates a fingerprint of monsoonal precipitation in the Eastern Himalaya from June to September (Figure 3). Average streamflow measured at the Majhitar station averaged 256.2 m³/s annually during the same period, whereas the monsoon months had an average streamflow of 573 m³/s. Snow cover depletion curves for the Tamor River basin indicate that the highest elevation zone (above 5500 m) had a maximum ~85% snow-covered area for the 2002–2006 period, dropping to ~73% during summer (Figure 4). The elevation zone between 4000 and 5550 m had an annual

maximum snow cover of ~40% with summer zonal snow coverage falling to ~12%. Elevations up to 4000 m had on average ~9% annual maximum snow cover.

Model parameterization

When the prior ranges of the parameters were deliberately set to be large, the model calibrated well with a good fit between the observed and modelled streamflow; however, this also resulted in several models with similar performance and physically implausible coefficients. Logically constraining the prior parameter ranges provided models with better fit and parameters that were physically plausible when varied across seasons and elevations. The posterior distributions of parameters after the MCMC optimization for all parameters for the 2002–2003 hydrological years are shown in Figure 5. When the model was optimized using the MCMC approach, some of the most sensitive parameters (such as x and y coefficients, critical temperature and lapse rate) exhibited a narrow, unimodal distribution with their ranges significantly reduced from the initial parameter ranges. The x and y coefficients required to compute the recession coefficient were the most sensitive parameters, as they determined the structure of hydrograph recession and corresponding proportion of daily melt water that appeared

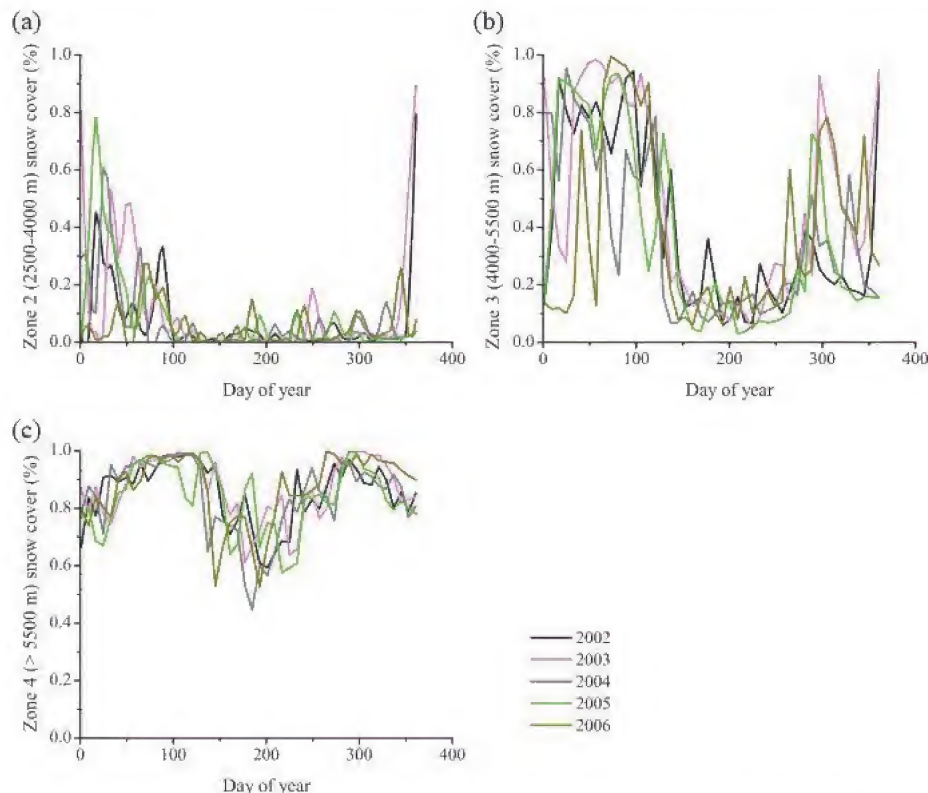


Figure 4. Snow cover depletion curves from the Moderate Resolution Imaging Spectroradiometer 8-day maximum snow cover 500-m resolution product in the Tamor River basin from 2002 to 2006 in (a) zone 2, elevation range from 2500–4000 m, (b) zone 3, elevation range from 4000–5500 m and (c) zone 4, elevation range greater than 5500 m.

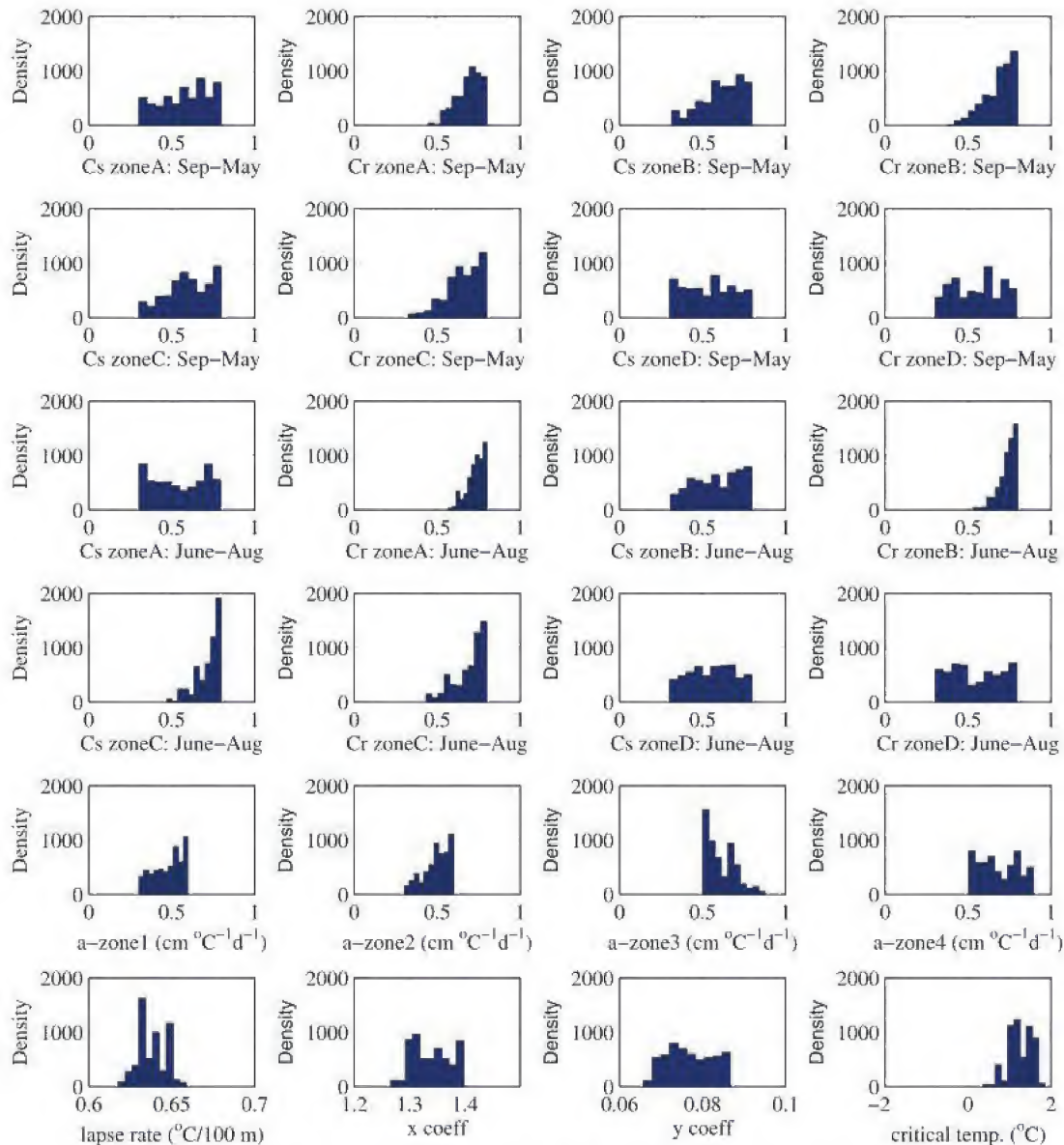


Figure 5. Posterior parameter distributions for the 2002–2003 hydrological years as histograms

immediately in the runoff. This shows that the MCMC approach performs well in constraining the most sensitive parameters of the model. Once a narrow posterior distribution is established for the sensitive parameters during the MCMC approach, changing other parameters does not result in a significant increase in model performance. Therefore, some of the remaining parameters such as snowmelt and rainfall runoff coefficients exhibited broad posterior distributions, and large standard deviations where good simulations of the observed streamflow were obtained over broad ranges (Figure 5 and Table III). The posterior distributions of runoff coefficients for both rainfall and snowmelt are comparable across types of precipitation and all simulated years. These coefficients represent the fraction of liquid water, from either snowmelt or rainfall,

that contributes to runoff and are expected not to vary as much across types of precipitation. Some of the observed differences in these coefficients within a single zone could be a result of the trade-off among parameters after the most sensitive parameters have been constrained well. Inadequate precipitation data from higher elevations zones in the mountainous regions further hindered our ability to constrain the runoff coefficients. Parameter estimates tend to be stable across years, though T_{crit} showed large variation, but also had a large spread. Degree-day factor estimates tended to be the highest for elevations greater than 4000 m (zones 3 and 4), which had the highest fraction of snow-covered area. The peaks in posterior distributions for the degree-day factor correspondingly rise from zone 1 to zone 3 elevation ranges.

Table III. Mean and standard deviation of parameters from the posterior distribution

Parameter		Mean and standard deviation of parameter across zones				
		Year	Zone 1 (533–2500 m)	Zone 2 (2500–4000 m)	Zone 3 (4000–5500 m)	Zone 4 (>5500 m)
Cs	June–August	2002	0.55 ± 0.15	0.59 ± 0.13	0.72 ± 0.07	0.56 ± 0.13
		2003	0.46 ± 0.13	0.44 ± 0.11	0.47 ± 0.12	0.52 ± 0.15
		2004	0.54 ± 0.14	0.54 ± 0.14	0.68 ± 0.11	0.55 ± 0.14
		2005	0.55 ± 0.14	0.55 ± 0.15	0.69 ± 0.11	0.55 ± 0.15
		2002	0.58 ± 0.14	0.61 ± 0.11	0.59 ± 0.13	0.54 ± 0.15
	September–May	2003	0.60 ± 0.14	0.56 ± 0.13	0.71 ± 0.07	0.56 ± 0.15
		2004	0.70 ± 0.09	0.71 ± 0.07	0.67 ± 0.11	0.54 ± 0.14
		2005	0.59 ± 0.14	0.43 ± 0.11	0.40 ± 0.08	0.54 ± 0.14
		2002	0.73 ± 0.05	0.74 ± 0.05	0.69 ± 0.09	0.55 ± 0.15
		2003	0.67 ± 0.11	0.56 ± 0.13	0.54 ± 0.15	0.54 ± 0.14
Cr	June–August	2004	0.71 ± 0.05	0.68 ± 0.09	0.59 ± 0.14	0.55 ± 0.14
		2005	0.76 ± 0.04	0.74 ± 0.08	0.76 ± 0.05	0.56 ± 0.14
	September–May	2002	0.69 ± 0.07	0.68 ± 0.09	0.65 ± 0.10	0.55 ± 0.14
		2003	0.37 ± 0.07	0.43 ± 0.09	0.40 ± 0.08	0.54 ± 0.14
		2004	0.71 ± 0.07	0.70 ± 0.08	0.54 ± 0.14	0.56 ± 0.14
		2005	0.69 ± 0.07	0.70 ± 0.08	0.72 ± 0.07	0.51 ± 0.13
	Annual	2002	0.48 ± 0.08	0.50 ± 0.0	0.61 ± 0.08	0.68 ± 0.102
		2003	0.42 ± 0.08	0.41 ± 0.08	0.79 ± 0.0	0.69 ± 0.11
		2004	0.53 ± 0.05	0.53 ± 0.06	0.81 ± 0.05	0.70 ± 0.2
		2005	0.45 ± 0.09	0.44 ± 0.09	0.80 ± 0.08	0.71 ± 0.12
LR	Annual	2002	0.64 ± 0.01			
		2003	0.51 ± 0.01			
		2004	0.68 ± 0.01			
		2005	0.54 ± 0.01			
Tcrit	Annual	2002	1.26 ± 0.28			
		2003	1.16 ± 0.49			
		2004	1.83 ± 0.13			
		2005	0.94 ± 0.62			
x coefficient	Annual	2002	1.34 ± 0.03			
		2003	1.26 ± 0.01			
		2004	1.29 ± 0.02			
		2005	1.11 ± 0.01			
y coefficient	Annual	2002	0.08 ± 0.01			
		2003	0.06 ± 0.01			
		2004	0.07 ± 0.01			
		2005	0.03 ± 0.01			

Cs, snowmelt runoff coefficient; Cr, rainfall runoff coefficient; a, degree day factor; LR, lapse rate.

The SRM is usually calibrated manually where known ranges of parameter values are maintained while changing other parameters by trial and error. This type of calibration can be inefficient in exploring the parameter space and resulted in an average NS statistic of 0.64 and volume difference of 10% across all simulated years for this study. Model calibration using MCMC optimization had a greater overall improvement with NS statistic of ~0.84 averaged across all simulated years. Figure 6 (a, c, e and g) shows the modelled streamflow against observed streamflow using the MCMC approach for four hydrological years (utilizing observed precipitation at the Lungthung station). The SRM is able to capture the daily streamflow in the annual hydrology of the basin; however, the model underestimates high discharge events, particularly during the monsoonal

months. Across all simulated years, the observed and modelled streamflow show a linear association with some bias during high discharge periods [Figure 6 (b, d, f and h)]. The model simulated streamflows have a higher NS statistic in the years where the summer peak discharge is lower relative to other years (Table IV and Figure 6).

Model sensitivity and uncertainty

The results of the experiment runs indicate that with the snowmelt runoff coefficients (Cs) set to zero, the model optimized as well as when Cs values were also included through the MCMC technique. The rainfall runoff coefficients (Cr) are parameterized to higher values, and the model is able to simulate the hydrograph by optimizing x and y coefficients with model performance equivalent to that

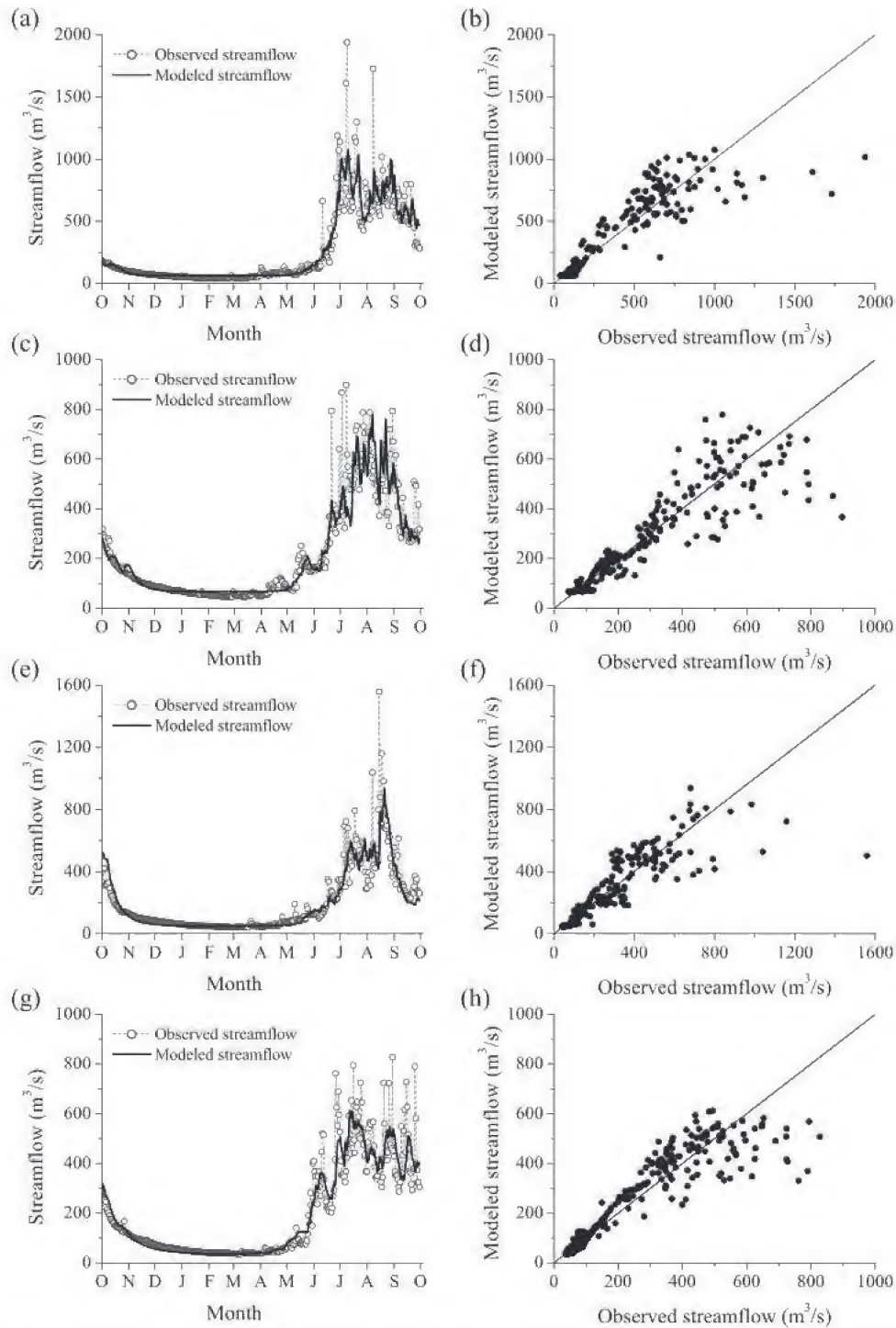


Figure 6. Time series and scatter plots of observed and modelled streamflow using observed precipitation at Lungthung station for 2002–2003 (a, b), 2003–2004 (c, d), 2004–2005 (e, f) and 2005–2006 (g, h)

with the best estimates of parameters as in Table IV. The first ensemble parameter sets (best ensemble) randomly selected from the posterior distribution output from MCMC did not exhibit any significant variations in model fit and performance. This is to be expected as the parameter sets are

accepted by the MCMC approach. Because the most sensitive parameters have narrow, unimodal distributions, similar model fit and performance is achieved within a broad distribution of other parameters. However, when the distribution of the most sensitive parameters was altered

Table IV. Evaluation of snowmelt runoff model performance with Markov Chain Monte Carlo technique and using observed precipitation at Lungthung station and gridded Asian Precipitation – Highly Resolved Observational Data Integration towards Evaluation precipitation data

Hydrological Year	Model efficiency (with observed precipitation)			Model efficiency (with APHRODITE precipitation)		
	Nash–Sutcliffe metric	Coefficient of determination	Difference of volume (D_v %)	Nash–Sutcliffe metric	Coefficient of determination	Difference of volume (D_v %)
2002–2003	0.84	0.84	1.9	0.73	0.79	13.1
2003–2004	0.85	0.85	5.2	0.82	0.87	11.9
2004–2005	0.80	0.80	2.7	0.78	0.80	5.10
2005–2006	0.87	0.87	0.7	0.85	0.85	3.12

APHRODITE, Asian Precipitation – Highly Resolved Observational Data Integration towards Evaluation.

slightly from their posterior distributions in the second ensemble parameter sets, there were notable changes in the model fit of the ensemble runs. Changing the x parameter randomly within $\pm 5\%$ of its mean value of its posterior distribution resulted in sizeable changes in model fit and performance (NS ranges from 0.3–0.8 and D_v ranges from $\square 6\%$ to 12%). Similarly, changing the y parameter also resulted in notable changes in model fit and performance (NS ranges from 0.7–0.8 and D_v ranges from $\square 8\%$ to 7%).

When the parameter distributions are altered randomly within $\pm 10\%$ of mean value of the posterior distribution, degree-day factor and critical temperature did not affect the model fit and total input contributions relative to the best ensemble. When lapse rate was varied within $\pm 10\%$ of mean value of its distribution, the average total input contributions of snowmelt were $25.8 \pm 4.4\%$, $4.2 \pm 1.9\%$ for precipitation as snow on previously snow-free areas, and $70.0 \pm 5.8\%$ for contributing precipitation across the 2002–2006 period. Figure 7a shows a larger 5th and 95th percentile envelope for simulated streamflows using lapse rate, indicative of the model's sensitivity to this parameter relative to the narrower envelope for critical temperature in Figure 7b.

The final ensemble runs where the parameters are randomly sampled from the cumulative distribution curve capture the uncertainty over the full range of parameter variations from the posterior distribution. Figure 8 shows the uncertainty bounds from the ensemble streamflow, which are large enough during the spring snowmelt period to include most of the observations but not large enough particularly during the summer monsoon months. The final ensemble streamflow simulations were also used to generate average total input contributions of rainfall and snowmelt for all simulated years and standard errors of these contributions (Figure 9). The average proportion of snowmelt in the runoff in the Tamor River basin for the 2002–2006 period is $29.7 \pm 2.9\%$, which includes $4.2 \pm 0.9\%$ from new snow onto previously snow-free areas, whereas $70.3 \pm 2.6\%$ is attributed to rainfall contributions. The cumulative runoff indicates that most of the snowmelt contribution occurs between April and August. Although there is interannual variability in the contribution of snowmelt runoff, elevation zone 3 (4000–5500 m) contributes on average $56.9 \pm 3.6\%$ of all snowmelt input and $28.9 \pm 1.1\%$ of all rainfall contribution to runoff. Elevation

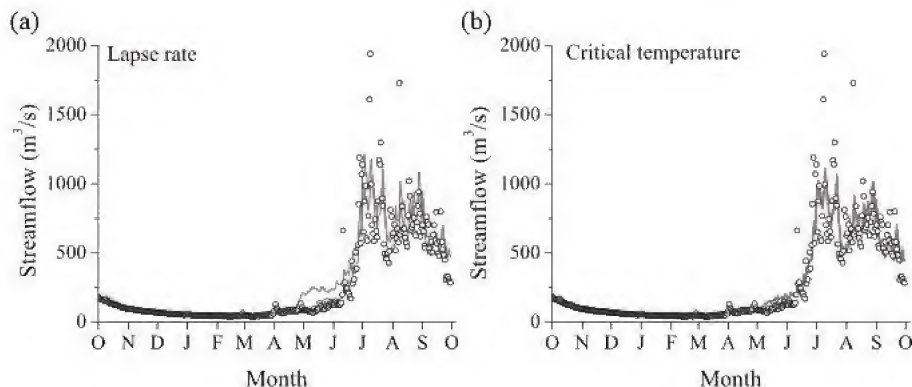


Figure 7. Streamflow ensemble simulations (2002–2003) by randomly varying the distribution of the parameters by $\pm 10\%$ of its mean posterior distribution. Black circles are observations and the dark cyan lines depict the 5th and 95th percentiles of the ensemble. Where lines for the 5th and 95th percentiles overlap only a single line is visible

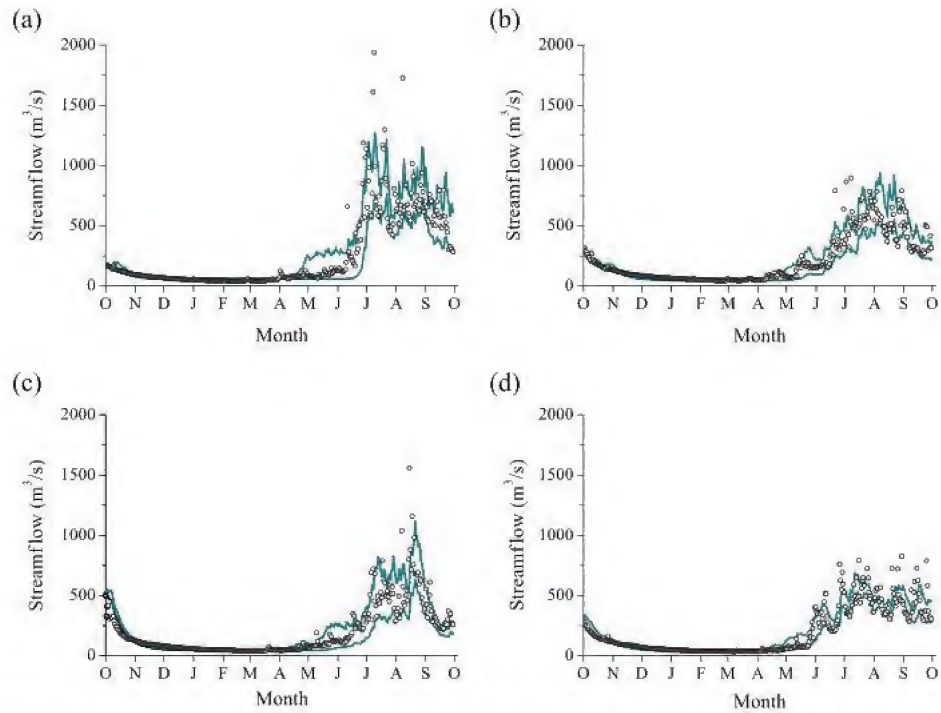


Figure 8. Streamflow ensemble simulations using observed precipitation at Lungthung station for Tamor River basin for hydrologic years (a) 2002–2003, (b) 2003–2004, (c) 2004–2005 and (d) 2005–2006. Black circles are observations and the cyan lines depict the 5th and 95th percentiles from the ensemble

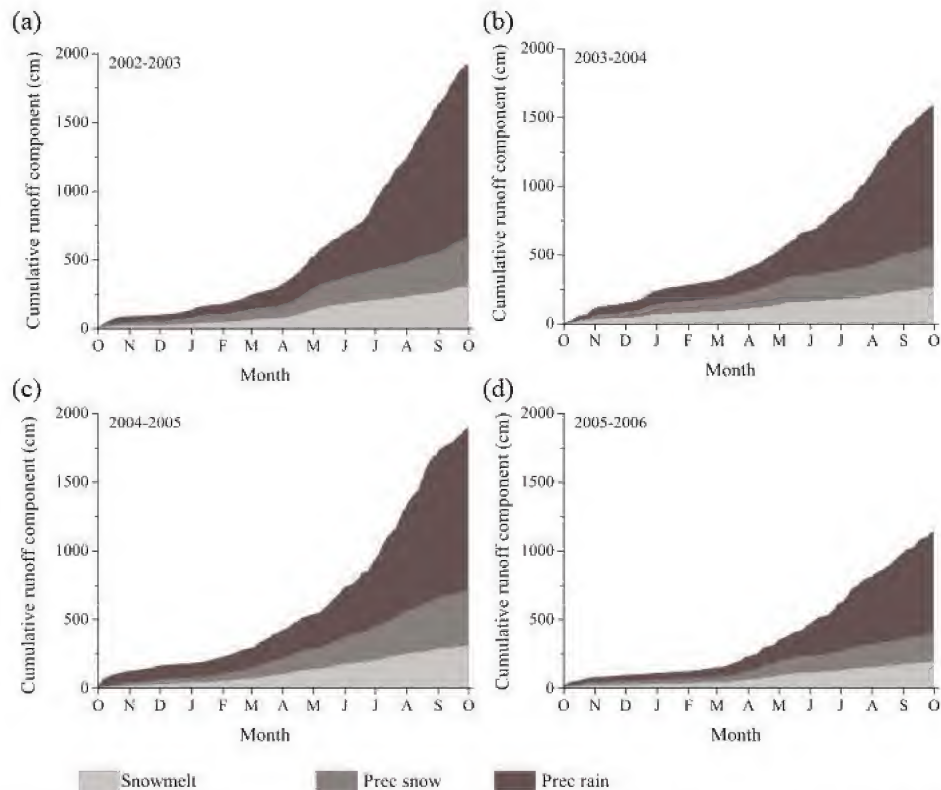


Figure 9. Cumulative curves of computed daily snowmelt depth, melted precipitation in the form of snow and rainfall depths for the (a) 2002–2003, (b) 2003–2004, (c) 2004–2005 and (d) 2005–2006 hydrological years for the Tamor basin

zones 1 (533–2500 m) and 2 (2500–4000 m) contribute on average $67.9 \pm 2.7\%$ of the all annual rainfall input to the basin.

Model results using APHRODITE precipitation

The modelled streamflow obtained using APHRODITE precipitation data over the hydrological periods and

calibrated using MCMC captured the observed streamflow fairly well (Figure 10). Modelled streamflow using observed station precipitation is also plotted alongside, which performs better on the basis of evaluation metrics and simulation of peak discharges (Table IV). Although the NS coefficient value was ~ 0.80 on average across all simulations, the model failed to capture peak discharge

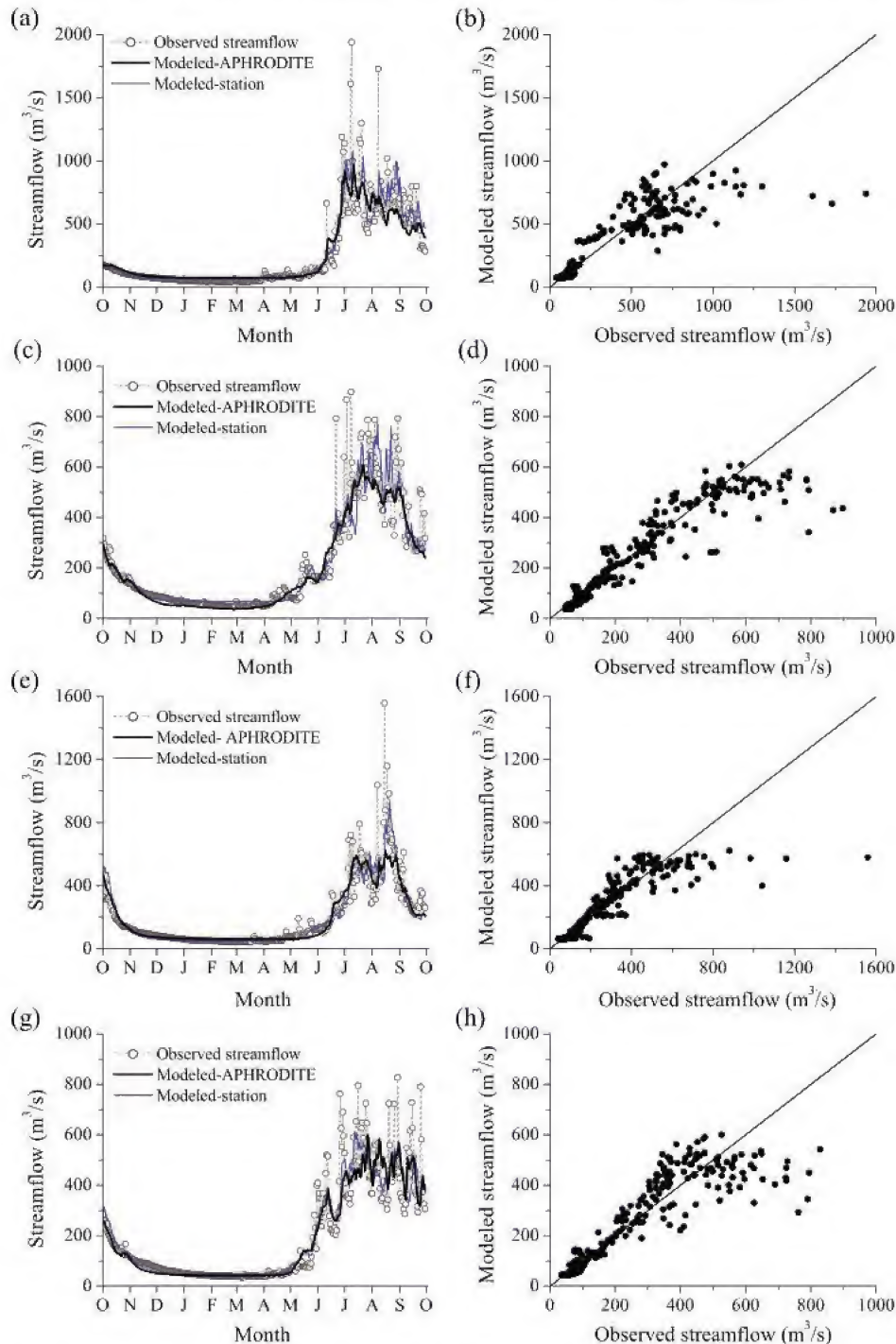


Figure 10. Time series and scatterplots of observed and modelled streamflow using Asian Precipitation – Highly Resolved Observational Data Integration towards Evaluation precipitation (black) and observed station precipitation (blue) for 2002–2003 (a, b), 2003–2004 (c, d), 2004–2005 (e, f) and 2005–2006 (g, h)

periods contributing to difference in volume (D_v) of on average 8.3%. Generally, the modelled hydrology using basin-averaged APHRODITE precipitation failed to capture high discharge periods across all years when compared to the simulations using gauged precipitation as input data. Overall, use of the APHRODITE precipitation data yielded similar model skill in simulating the hydrograph but estimated a smaller total contribution from precipitation input to the basin (more from snowmelt) when compared with model simulations using the observed station precipitation data.

DISCUSSION

This study provides an application and evaluation of the SRM in a mountainous basin in the eastern Nepalese Himalaya. In this study, the SRM was coupled to a MCMC data assimilation approach to examine associated parameter sensitivities, uncertainties and model performance in the Tamor River basin for the 2002–2006 period. A majority of the studies involving snowmelt runoff models use parameter values from existing studies, and therefore, parameter calibration, types of input data and equifinality in parameter sets have not been fully explored (particularly for the Himalayan region). Additionally, lack of observational data is problematic for transfer of parameters across space and time and may introduce added uncertainty. Uncertainty in a model is usually a joint outcome of uncertainties in model structure, input data errors and parameter errors, which leads to difficulty in approximating the behaviour of a model consistently (Vrugt *et al.*, 2005). Although any parameter optimization technique can only reduce uncertainty in the parameters, optimization and data assimilation methods such as the MCMC may be better for accounting important sources of uncertainty.

Overall, parameter optimization using MCMC increased the fit between the observed and modelled streamflows and further reduced the volume difference error. This study also showed that prior ranges of parameter values are important in constraining model performance and decreasing parameter uncertainty. When the parameter ranges were logically constrained or informed from estimates from previous studies and then optimized using MCMC, the output parameters value ranges were more relevant and physically plausible. Model evaluation through additional experiment runs indicate that despite overall good performance of SRM, there might be lack of confidence in model structure in simulating physical realism of some of the processes. For instance, the model was able to reproduce the hydrograph well even when snowmelt runoff contributions were excluded from simulations. As the contributing rainfall to the Tamor basin is high, relative to the snow component, model parameters were able to compensate for the absence

of snowmelt contributions and simulate the annual hydrograph with relatively high fit and performance. This test identifies an important model structural uncertainty that is not currently reflected in the reported uncertainty on forecasts and the associated snowmelt contribution. It also identifies that the hydrograph does not constrain estimates of the fractional contributions of total outflow coming from snowmelt *versus* rainfall. Instead, the model's estimates of the snowmelt contribution derive mainly from volume considerations based on the snow-covered area, the degree-day model of melt and rainfall depths. This lends important new insight into the practical outcomes of SRM application that may not have been given full attention in past applications for similar purposes. This partly reflects a limitation of a conceptual lumped model such as the SRM. However, there are some clear advantages to using only a few parameters for modelling, particularly when there is such a lack of observations and strong seasonal variation in the nature of parameters across a topographically challenging environment. When more complex physically based hydrological models are applied to such environments, calibration can be further challenged owing to the large number of parameters involved. Furthermore, it is not clear that such an improvement in mechanistic realism would translate into improved model skill in matching the hydrograph or in representing volume contributions to total basin surface water outflow.

The posterior distribution output from MCMC indicates that the coupled approach was successful in constraining the ranges of sensitive parameters in the model. Model sensitivity using ensemble runs indicated that the x coefficient, y coefficient and lapse rate are the most sensitive parameters in the model. The recession coefficient (k), which is a function of x and y coefficients, is important as it represents an inertia or memory in streamflow and also controls the amount of the daily melt water that appears in the runoff, whereas lapse rate is important in lapsing the zonal temperature to compute daily zonal snowmelt depth. The narrow, unimodal distributions of these parameters provide an indication of the degree to which these parameters were constrained by the MCMC approach. Parameters that are well constrained tend to have small standard deviations with well-defined unimodal distributions, whereas poorly constrained parameters exhibit flat distributions with large standard deviations (Braswell *et al.*, 2005). Once the sensitive parameters are constrained to a narrow distribution, other parameters that are not as sensitive provide a similar model fit and performance resulting in broad posterior ranges. A study by Seibert (1997) also found that only few of the parameters were well defined when the Hydrologiska Byråns Vattenbalansavdelning model, a conceptual degree-day model, was parameterized over central Sweden. This is also suggestive of trade-offs among parameters leading to broader posterior distributions where different parameter

sets may be acceptable in reproducing the observed hydrology within a basin.

The overall model parameter uncertainty was characterized as standard errors in the total input contributions and uncertainty in time history of streamflow as 5% and 95% confidence intervals (Figure 8). Because the uncertainty bounds are not large enough to include all of the observations, parameter uncertainty alone cannot explain the total error in the model. If the bounds were large enough, parameter variability alone could account for overall uncertainty by compensating other sources of error introduced by model structure and input data (Blasone *et al.*, 2008). As most of the observations outside of the uncertainty bounds are during the summer months, the unaccounted uncertainty could arise from uncertainty in input precipitation data.

On the basis of the evaluation metrics, use of APHRODITE gridded precipitation product provided comparable skill relative to the discharge modelled using observed station observations. APHRODITE data have been shown to be effective in simulating and forecasting discharges using a snowmelt model in other high-altitude ranges such as the Karakoram region (Tahir *et al.*, 2011). The results indicate that the total rainfall contributions to runoff is lower when APHRODITE is used for calibrating the model. This is consistent with past studies that indicated underestimated total annual precipitation and high discharges when APHRODITE was used in snowmelt runoff modelling in the Hunza River basin (Tahir *et al.*, 2011). Nonetheless, the findings from our study using APHRODITE indicate that these data can be important inputs for precipitation in basins lacking ground observations. We also find, however, that uncertainties in the available input data such as precipitation are equally as important as uncertainty introduced by model parameters. Model parameters calibrated using an input precipitation that either underestimates or overestimates actual precipitation will compensate for such error when matching the hydrograph (Pellicciotti *et al.*, 2012) but may still alter conclusions about fractional contributions from snowmelt and rain.

This study shows a total snowmelt contribution to be $29.7 \pm 2.9\%$ of annual discharge averaged across the 2002–2006 hydrological years for the Tamor basin. Bookhagen and Burbank (2010) showed that Eastern Himalayan catchments draining into the Bay of Bengal received ~80% of their annual rainfall during monsoon and less than 20% from snowmelt. For comparison, snowmelt contributions to annual runoff in the Satluj basin (22 275 km²) in the western Himalayan region has been estimated to be up to ~59%, with the summer contributions averaging ~75% for the late 1980s period (Singh and Jain, 2003). Another study modelling snow and glacial melt in the Dudh Kosi River basin (3712 km²) estimated total melt contributions to be 34% (Nepal *et al.*, 2013). This study also

found the 4000–5500 m elevation range to be the most important with regard to its snowmelt contributions to annual runoff. Biggs and Whitaker (2012) also introduced the concept of critical zone using the example of Merced River basin, California, which can be important in anticipating the impacts of regional climate change on the timing and volume of runoff events.

A logical incremental improvement on this work would be to incorporate the present and future role of glaciers in the runoff. Previous studies in the Himalayan region (e.g. Tahir *et al.*, 2011) have used the SRM to include glacier melt by calibrating the model using a higher degree-day factor for the higher elevations. Although this SRM study does not explicitly incorporate glaciated regions, they are partly taken into account through the use of snow depletion curves. The decline of snow cover depletion curves levels out during the later portion of the snowmelt season, thereby indicating the presence of permanent snow or glaciers (e.g. zone 4). Model modifications would involve incorporation of glacier-covered areas at the highest elevations and calibration of model for parameters such as degree-day factor that are different for snow and ice. Additional input data such as estimates of snow cover data, calibration against multiple variables such as inclusion of glacier mass balances or fixing known parameters from field observations are usually the options to further narrow the posterior distributions and better constrain these parameters that vary seasonally across elevations (Boudhar *et al.*, 2009; Pellicciotti *et al.*, 2012). Given the limited availability of data and the parsimoniousness of this snowmelt runoff model, obtaining values through field observations or fixing parameters based on values reported from previous short field campaigns are potential options to improve the model.

SUMMARY

This study has shown that a snowmelt runoff model based on degree-day factors has skill in simulating daily streamflow in a mountainous environment with limited coverage of hydrometeorological measurements. Coupling the SRM with an MCMC method provided an improved fit to observed streamflows but still failed to capture peak discharge during the summer monsoon months. This is likely due in part to the lack of precipitation data coverage throughout the basin but could also result from model structural errors. Model performance in simulating the hydrograph is strongly sensitive to recession coefficients and the lapse rate, but exhibited little sensitivity to runoff coefficients, the critical temperature that determines the phase of precipitation (snow or rain) and the degree-day factor that estimates melt depth from degree days. Correspondingly, the MCMC approach to parameter determination yielded narrow distributions only for those

parameters to which the model-estimated hydrograph is sensitive. The study provides a useful guide for how to constrain parameters, provide uncertainty bounds in snowmelt contributions to runoff, analyze effects of input precipitation and examine model uncertainty in Himalayan basins. The Himalayan terrain, meteorological conditions and lack of ground-based observations continue to challenge snowmelt runoff and hydrologic modelling in the region. By testing results with two alternative precipitation datasets, we noted how both the available input data and the parameter sets introduce uncertainties, and methods to thoroughly characterize and minimize these uncertainties is important. The need for further hydrological research on snow and glacial melt and, moreover, strengthening of hydrometeorological observation network for the HKH region should not be overlooked. Overall, this study shows that a combination of known parameter ranges along with an iterative model-data fusion technique such as the MCMC can provide a calibration and optimization method to explore the parameter space efficiently, obtain reliable parameter estimates and quantify uncertainty in model results and associated inferences.

ACKNOWLEDGEMENTS

This research was funded in part by a NASA Earth and Space Science Fellowship (Grant No. NNX10AO65H). We would like to thank the Department of Hydrology and Meteorology, Government of Nepal for providing hydrometeorological data used in this study. We thank Dr. Trent Biggs and one anonymous reviewer for their constructive comments.

REFERENCES

- Adam JC, Hamlet AF, Lettenmaier DP. 2009. Implications of global climate change for snowmelt hydrology in the twenty-first century. *Hydrological Processes* **23**: 962–972.
- Akhtar M, Ahmad N, Booij MJ. 2008. The impact of climate change on the water resources of Hindukush–Karakorum–Himalaya region under different glacier coverage scenarios. *Journal of Hydrology* **355**: 148–163.
- Andermann C, Bonnet S, Gloaguen R. 2011. Evaluation of precipitation data sets along the Himalayan front. *Geochemistry, Geophysics, Geosystems* **12**: Q07023.
- Barnett TP, Adam JC, Lettenmaier DP. 2005. Potential impacts of a warming climate on water availability in snow-dominated regions. *Nature* **438**: 303–309.
- Beven K, Freer J. 2001. Equifinality, data assimilation, and uncertainty estimation in mechanistic modelling of complex environmental systems using the GLUE methodology. *Journal of Hydrology* **249**: 11–29.
- Biggs TW, Whitaker T. 2012. Critical elevation zones of snowmelt during peak discharges in a mountain river basin. *Journal of Hydrology* **438–439**: 52–65.
- Blasone RS, Vrugt JA, Madsen H, Rosbjerg D, Robinson BA, Zyvoloski GA. 2008. Generalized likelihood uncertainty estimation (GLUE) using adaptive Markov Chain Monte Carlo sampling. *Advances in Water Resources* **31**: 630–648.
- Bolch T, Kulkarni A, Kääb A, Huggel C, Paul F, Cogley J, Frey H, Kargel J, Fujita K, Scheel M. 2012. The state and fate of Himalayan glaciers. *Science* **336**: 310–314.
- Bookhagen B, Burbank DW. 2010. Towards a complete Himalayan hydrologic budget: the spatiotemporal distribution of snow melt and rainfall and their impact on river discharge. *Journal of Geophysical Research* **115**: F03019.
- Boudhar A, Hanich L, Boulet G, Duchemin B, Berjamy B, Chehbouni A. 2009. Evaluation of the snowmelt runoff model in the Moroccan High Atlas mountains using two snow-cover estimates. *Hydrological Sciences Journal* **54**: 1094–1113.
- Braswell BH, Sacks WJ, Linder E, Schimel DS. 2005. Estimating diurnal to annual ecosystem parameters by synthesis of a carbon flux model with eddy covariance net ecosystem exchange observations. *Global Change Biology* **11**: 335–355.
- Braun LN, Grabs W, Rana B. 1993. Application of a conceptual precipitation-runoff model in Langtang Khola Basin, Nepal Himalaya. *Snow and Glacier Hydrology* **218**: 221–237.
- Butt MJ, Bilal M. 2011. Application of snowmelt runoff model for water resource management. *Hydrological Processes* **25**: 3735–3747.
- Clark MP, Slater AG, Barrett AP, Hay LE, McCabe GJ, Rajagopalan B, Leavesley GH. 2006. Assimilation of snow covered area information into hydrologic and land-surface models. *Advances in Water Resources* **29**: 1209–1221.
- Duncan J, Biggs EM. 2012. Assessing the accuracy and applied use of satellite-derived precipitation estimates over Nepal. *Applied Geography* **34**: 626–638.
- Gautam R, Hsu NC, Lau KM. 2010. Pre-monsoon aerosol characterization and radiative effects over the Indo-Gangetic plains: implications for regional climate warming. *Journal of Geophysical Research* **115**: D17208.
- Gurtz J, Lang H, Verbunt M, Zappa M. 2005. The use of hydrological models for the simulation of climate change impacts on mountain hydrology. In *Global Change and Mountain Regions: An Overview of Current Knowledge*, Huber UM, Bugmann HKM, Reasoner MA (eds). Springer: Dordrecht, Netherlands.
- Hall DK, Riggs GA, Salomonson VV, DiGirolamo NE, Bayr KJ. 2002. MODIS snow-cover products. *Remote Sensing of Environment* **83**: 181–194.
- Hall DK, Salomonson VV, Riggs GA. 2006. *MODIS/Terra Snow Cover 8-Day L3 Global 500m Grid*. National Snow and Ice Data Center: Version 5. Boulder, Colorado USA.
- Hock R. 2003. Temperature index melt modelling in mountain areas. *Journal of Hydrology* **282**: 104–115.
- Immerzeel WW, Beek LPHv, Bierkens MFP. 2010. Climate change will affect the Asian water towers. *Science* **328**: 1382–1385.
- Immerzeel WW, van Beek LPH, Konz M, Shrestha A, Bierkens MFP. 2011. Hydrological response to climate change in a glacierized catchment in the Himalayas. *Climatic Change* **110**: 721–736.
- IPCC. 2007. Climate change 2007: synthesis report. Team CW, Pachauri RK, Reisinger A (eds).
- Konz M, Uhlenbrook S, Braun L, Shrestha A, Demuth S. 2007. Implementation of a process-based catchment model in a poorly gauged, highly glacierized Himalayan headwater. *Hydrology and Earth System Sciences* **11**: 1323–1339.
- Martinez J, Rango A, Roberts R. 2008. *Snomelt Runoff Model (SRM) User's Manual*. Gomez-Landsea E, Bleiweiss MP (eds). New Mexico State University, Las Cruces, New Mexico.
- Maurer E, Adam J, Wood A. 2009. Climate model based consensus on the hydrologic impacts of climate change to the Rio Lempa basin of Central America. *Hydrology and Earth System Sciences* **13**: 183–194.
- McLaughlin D, O'Neill A, Derber J, Kamachi M. 2005. Opportunities for enhanced collaboration within the data assimilation community. *Quarterly Journal of the Royal Meteorological Society* **131**: 3683–3693.
- Messerli B, Viroli D, Weingartner R. 2004. Mountains of the world: vulnerable water towers for the 21st century. *Ambio, Special Report Number 13* **13**: 29–34.
- Metropolis N, Rosenbluth AW, Rosenbluth MN, Teller AH, Teller E. 1953. Equation of state calculations by fast computing machines. *The journal of chemical physics* **21**: 1087–1092.
- Mishra S. 2009. Uncertainty and sensitivity analysis techniques for hydrologic modeling. *Journal of hydroinformatics* **11**: 282–296.
- Nepal S, Krause P, Flügel WA, Fink M, Fischer C. 2013. Understanding the hydrological system dynamics of a glaciated alpine catchment in the

- Himalayan region using the J2000 hydrological model. *Hydrological Processes*, DOI: 10.1002/hyp.9627
- Panday PK, Frey KE, Ghimire B. 2011. Detection of the timing and duration of snowmelt in the Hindu Kush-Himalaya using QuikSCAT, 2000-2008. *Environmental Research Letters* **6**: 1-13.
- Panday P, Thibeault J, Frey K. in review. A multi-model analysis of changing climate in the Hindu Kush-Himalayan region using CMIP3 projections for temperature and precipitation. *International Journal of Climatology*.
- Pellicciotti F, Buerger C, Immerzeel WW, Konz M, Shrestha AB. 2012. Challenges and uncertainties in hydrological modeling of remote Hindu Kush-Karakoram-Himalayan (HKH) basins: suggestions for calibration strategies. *Mountain Research and Development* **32**: 39-50.
- Seibert J. 1997. Estimation of parameter uncertainty in the HBV model. *Nordic Hydrology* **28**: 247-262.
- Shrestha R, Takara K, Tachikawa Y, Jha RN. 2004. Water resources assessment in a poorly gauged mountainous catchment using a geographical information system and remote sensing. *Hydrological Processes* **18**: 3061-3079.
- Singh P, Jain S. 2003. Modelling of streamflow and its components for a large Himalayan basin with predominant snowmelt yields. *Hydrological Sciences Journal* **48**: 257-276.
- Smith TJ, Marshall LA. 2008. Bayesian methods in hydrologic modeling: a study of recent advancements in Markov Chain Monte Carlo techniques. *Water Resources Research* **44**: W00B05.
- Sun W, Ishidaira H, Bastola S. 2012. Calibration of hydrological models in ungauged basins based on satellite radar altimetry observations of river water level. *Hydrological Processes* **26**: 3524-3537.
- Tahir AA, Chevallier P, Arnaud Y, Neppel L, Ahmad B. 2011. Modeling snowmelt-runoff under climate scenarios in the Hunza River basin, Karakoram Range, Northern Pakistan. *Journal of Hydrology* **409**: 104-117.
- Vrugt JA, Diks CGH, Gupta HV, Bouten W, Verstraten JM. 2005. Improved treatment of uncertainty in hydrologic modeling: combining the strengths of global optimization and data assimilation. *Water Resources Research* **41**: W01017.
- WMO. 1986. Intercomparison of models of snowmelt runoff. In: Operational Hydrology Report World Meteorological Institution (WMO), Geneva, Switzerland.
- Yao T, Thompson L, Yang W, Yu W, Gao Y, Guo X, Yang X, Duan K, Zhao H, Xu B. 2012. Different glacier status with atmospheric circulations in Tibetan Plateau and surroundings. *Nature Climate Change* **2**: 663-667.
- Yatagai A, Arakawa O, Kamiguchi K, Kawamoto H, Nodzu MI, Hamada A. 2009. A 44-year daily gridded precipitation dataset for Asia based on a dense network of rain gauges. *Sola* **5**: 137-140.
- Zobitz J, Desai A, Moore DJP, Chadwick M. 2011. A primer for data assimilation with ecological models using Markov Chain Monte Carlo (MCMC). *Oecologia*: **167**: 599-611.